

Article

Not peer-reviewed version

Cotton Swab-Based SERS Substrate for Ultrasensitive Detection with Year-Long Stability and Multiple Recyclability

[Minh Hoang Tran](#)^{*}, Anh Duc Luong, Chi Linh Thao Nguyen, Minh Duy Hoang, [Tran Van Khai](#)

Posted Date: 31 January 2025

doi: 10.20944/preprints202501.2345.v1

Keywords: ultrasensitive SERS; hybrid nanomaterial; plasmonic material; graphene oxide; flexible substrate; cotton swab; stability; recyclability



Preprints.org is a free multidisciplinary platform providing preprint service that is dedicated to making early versions of research outputs permanently available and citable. Preprints posted at Preprints.org appear in Web of Science, Crossref, Google Scholar, Scilit, Europe PMC.

Copyright: This open access article is published under a Creative Commons CC BY 4.0 license, which permit the free download, distribution, and reuse, provided that the author and preprint are cited in any reuse.

Disclaimer/Publisher's Note: The statements, opinions, and data contained in all publications are solely those of the individual author(s) and contributor(s) and not of MDPI and/or the editor(s). MDPI and/or the editor(s) disclaim responsibility for any injury to people or property resulting from any ideas, methods, instructions, or products referred to in the content.

Article

Cotton Swab-Based SERS Substrate for Ultrasensitive Detection with Year-Long Stability and Multiple Recyclability

Minh H. Tran ^{*}, Anh D. Luong [†], Chi L. T. Nguyen [†], Minh D. Hoang and Khai V. Tran

Faculty of Materials Technology, Ho Chi Minh City University of Technology – Vietnam National University (HCMUT-VNU), 268 Ly Thuong Kiet Street, District 10, Ho Chi Minh City, Vietnam

^{*} Correspondence: mhtran@hcmut.edu.vn

[†] These authors contributed equally to this work.

Abstract: In recent years, the development of Surface Enhanced Raman Spectroscopy (SERS) substrates has seen significant advancement. In this research, we successfully fabricated cotton swab-based SERS substrates using a facile solution-based method. Our SERS substrates showed not only ultrasensitive detection capability but also impressive long-term stability and multiple recyclability rounds. In particular, we reported a detection limit of 10-12 M RhB and a detectable concentration of thiophanate methyl as low as 10-10 M using our cotton swab-based SERS substrates. The stability of our substrates reached a 12-month mark, and they were recycled as many as five times simply by cleaning them with ozone. We look forward to expanding the applicability of our cotton-swab based SERS substrates to various types of analytes as well as optimizing our cotton-swab based SERS substrates for longer stability and more recyclability.

Keywords: ultrasensitive SERS; hybrid nanomaterial; plasmonic material; graphene oxide; flexible substrate; cotton swab; stability; recyclability

1. Introduction

For almost five decades of research and development, Surface Enhanced Raman Spectroscopy (SERS) has emerged as one of the most powerful analytical techniques, reliable for several applications ranging from chemistry, food science, security, environmental science to biomedicine and more [1]. When compared with other conventional analytical techniques, such as high-performance liquid chromatography (HPLC) [2], gas chromatography-mass spectroscopy (GC/MS) [2], capillary electrochromatography (CE) [3], enzyme cycling assays [4], photoluminescence [5], and ion mobility spectrometry [6], which require expensive equipment and maintenance, time-consuming method development, or complicated sample pre-treatment techniques, SERS possesses several advantages. First, SERS is a fast and simple way to analyze samples. All you need are a metallic surface of SERS-active material and a Raman spectrometer system. The samples can be in their original forms without or with minimal pre-treatments. The substrates for SERS can be fabricated easily by simple chemical methods or can be manufactured in large-scale using inkjet technology [7]. Then the time from sample collecting onto the substrate to result reading is only the matter of minutes or even less than a minute [8]. Second, SERS is an analytical technique with such a high sensitivity that a decent number of publications have already reported single-molecule detection [9,10]. In addition, the structure of each analyte is associated with a single set of Raman peaks, thus such the identification based on molecular “fingerprint” is highly specific. Third, with the availability of handheld Raman spectrometer and the development of SERS substrates based on flexible or daily-use materials, SERS is becoming more mobile and versatile than ever. The mobility makes on-field detection feasible and the versatility means that it is possible to fabricate specific SERS substrates for

different applications. Consequently, the overall cost of SERS system can be reduced, making SERS a more affordable technique, which is also the fourth advantage.

The enhancement of Raman scattering by SERS is dominated by the electromagnetic effect caused by localized surface plasmon resonance (SPR) when laser is irradiated onto plasmonic surface [11]. Thus, several plasmonic materials have been experimented for SERS including Au [12], Ag [13], Cu [12], Pt [14], and Pd [15]. Likewise, a much weaker enhancement mechanism, the chemical mechanism, is believed to occur due to light-induced charge transfer between the analyte and the substrate leading to altered geometrical or electronic structure of the analyte [16]. Research on chemical mechanism has been intensively studied on several non-plasmonic materials such as graphene and its derivatives [16–18], few-layered MoO₃ nanosheets [19], GaN microrod array [20], and plasma-treated MoS₂ nanoflakes [21]. In applications, SERS materials can be fabricated as colloidal substrates [22], but most substrates are fabricated by patterning the surfaces of SERS materials [23,24] or by depositing them on supporting substrates such as glass [8,25] or Si [12,14]. Recently, more interests in flexible substrates to reduce cost and improve versatility and disposal have led to the development of SERS substrates based on plastics [26], textile [27], paper [7,27], or cotton swab [28,29]. Regardless of the fabrication techniques, in general, SERS substrates showed very impressive sensitivity with significantly high enhancement factors (EFs). For example, 10⁻⁷ M methimazole in synthetic urine was detected by colloidal Au nanostar substrates (EF ≈ 5.2 × 10⁵) [22]; inkjet-printed Au nanoparticles on paper was made into dipstick or swab that was capable of detecting 1,2-Bis(4-pyridyl)ethylene at concentration as low as 1.8 ppb [7] or highly dense sub-10-nm Ag nanogap arrays exhibited a calculated EF up to 10⁹ [23]. Comparably, non-plasmonic SERS substrates such as CVD grown MoO₃ nanosheets on SiO₂/Si or monolayer graphene also achieved limit of detection of 2 × 10⁻⁸ M R6G (EF ≈ 2.28 × 10⁴) [19] or 10⁻⁸ M protoporphyrin IX, respectively [17].

In our most recent publication [29], we utilized cotton swab as an inexpensive, flexible, and highly versatile supporting substrate for SERS-active Ag nanoparticles (Ag NPs). We proved that such a simple SERS substrate was capable of easily detecting down to 10⁻¹⁰ M RhB and an impressive EF exceeding 10¹⁰ was achieved. Furthermore, we added an overlay of graphene oxide (GO) on top of the cotton swab/Ag substrate to deliberately improve sensitivity by taking advantage of the greater analyte adsorption and the charge transfer mechanism of GO. Indeed, the combination of a plasmonic material with a non-plasmonic material to improve SERS sensitivity has already been studied by several groups. The selection of materials and their architectures has been many. For example, Au NPs or Ag NPs were grown directly *in situ* from reduced GO [30,31] or Ag NPs were decorated onto functionalized multiwalled carbon nanotubes [32]. Similarly, plasmonic noble metal was also combined with non-plasmonic metal oxide support such as Au layers sputtered onto ZnO nanoflowers [33], Ag NPs impregnated onto TiO₂ nanorods [34–36], or Ag film evaporated on top of self-assembled, three-dimensional SiO₂ nanosphere lattice [37]. In general, these combinations showed higher sensitivity as compared with single noble metals due to synergistic effects from the combined materials as well as the enhanced light scattering and additional hot spots from the surface structures. However, the constant exposure of noble metals to the surrounding media or reagents may cause unwanted degradation. Thus, another scheme in which the plasmonic material was covered by non-plasmonic material was explored. Some typical structures included few-layer-graphene covering Ag NPs [38], Cu@graphene core-shell NPs [39], or Ag@Fe₃O₄ core-shell nanospheres [40]. As a result, the protected SERS-active materials were able to last for several days to months.

In addition to performance and stability, recyclability of SERS substrates is another area of active research. To be recyclable, the general scheme was to combine the plasmonic metal with another material that was capable of degrading the analyte and prepared the substrate for a new round of detection. The most used supporting materials were the semiconductor metal oxides, TiO₂ or ZnO in particular, due to their photocatalytic properties under light irradiation. Singh *et al* successfully recycled SERS substrate from Ag-decorated TiO₂ nanorods six times by irradiating UV light at room

temperature for ~150 minutes to degrade R6G [35]. Similarly, He *et al* reported the recyclable detection of R6G and 2,4-D up to five cycles for Ag-decorated-ZnO-nanorod substrate by using UV light irradiation at room temperature for 30 to 500 minutes [41]. More interestingly, a report by Xu *et al* even indicated that irradiating visible light for two hours at room temperature was sufficient to degrade R6G and reuse Ag-decorated TiO₂ nanograss for at least three cycles [36] while another report by Weng *et al* showed that Fe₂O₃-Ag hybrid hollow microspheres were reused five times by simply irradiating visible light for 5 minutes to promote charge transfer between Ag NPs and Fe₂O₃ [42]. In addition to light, some authors suggested using ethanol to rinse SERS substrates, such as Ag@Fe₃O₄ core-shell nanospheres [40] or superhydrophobic microball/nanosheet Ag film [24]. In these cases, R6G and 4-ATP were washed away by ethanol and the like-new substrates were reused several times.

In this work, we continued our previous success on the fabrication of cotton swabs covered with Ag NPs and GO (Ag NPs/cotton swab & GO/Ag NPs/cotton swab) as flexible SERS substrates for ultrasensitive detection. In the first part, we described a few key results of our SERS substrate characterization. Then, we reported a detection limit of 10⁻¹² M for RhB and showed the applicability of our SERS substrates to detect highly toxic thiophanate methyl fungicide at ultra-low concentrations. Furthermore, the stability of Ag-covered cotton swab with and without GO, up to 12 months, would also be reported in this work. Last but not least, results from the recyclability of GO/Ag NPs/cotton swab would be described in this work as well, which presented a simple way to reuse the substrate. This is our second report about cotton-swab based SERS substrates to update our efforts toward developing a low-cost, high efficiency and durable SERS substrate.

2. Materials and Methods

2.1. Materials for SERS Substrate Fabrication

For the synthesis of Ag NPs, silver nitrate (AgNO₃, 99.8%) and sodium citrate dihydrate (Na₃C₆H₅O₇·2H₂O, 99%) were purchased from VWR (Radnor, PA, USA) and Merck (Darmstadt, Germany), respectively, and were used as received. Similarly, for the synthesis of GO, we used chemicals obtained from Merck (Darmstadt, Germany), which included graphite flakes (~5 μm, 99.8%), sulfuric acid (H₂SO₄, 98%), phosphoric acid (H₃PO₄, 85%), potassium permanganate (KMnO₄, 98%), hydrochloric acid (HCl, 5%) and hydrogen peroxide (H₂O₂, 30%) without any further treatment. Cotton swab which was purchased from a local supermarket was used as supporting substrate after a series of extensive cleaning steps in acetone, ethanol and DI water. (3-aminopropyl)trimethoxysilane (APTMS, 97%) from Energy Chemical (Zhejiang, China) was used as additive to activate cotton swab before deposition of Ag NPs. Finally, DI water was used to prepare all solutions in this study.

2.2. Characterization

In this paper, some selected characterization methods were used to verify the presence of Ag NPs and GO nanosheets as well as their distribution on cotton swab. In particular, scanning electron microscopic (SEM) images were taken by FESEM S4800 instrument (Hitachi, Japan) at 10 kV accelerating voltage to provide morphology, size and distribution details. Likewise, structural information of Ag NPs was obtained by x-ray diffraction (XRD) using a LabX XRD-6100 diffractometer (Shimadzu, Japan) equipped with a LYNXEYE XE-T detector, a vertical goniometer and a sealed Cu tube, while that of GO nanosheets was obtained by Raman spectroscopy using an XploRA Plus Raman Spectrometer (Horiba, UK).

2.3. Methods of SERS Substrate Fabrication

The processes of SERS substrate fabrication and performance tests are described schematically in Figure 1.

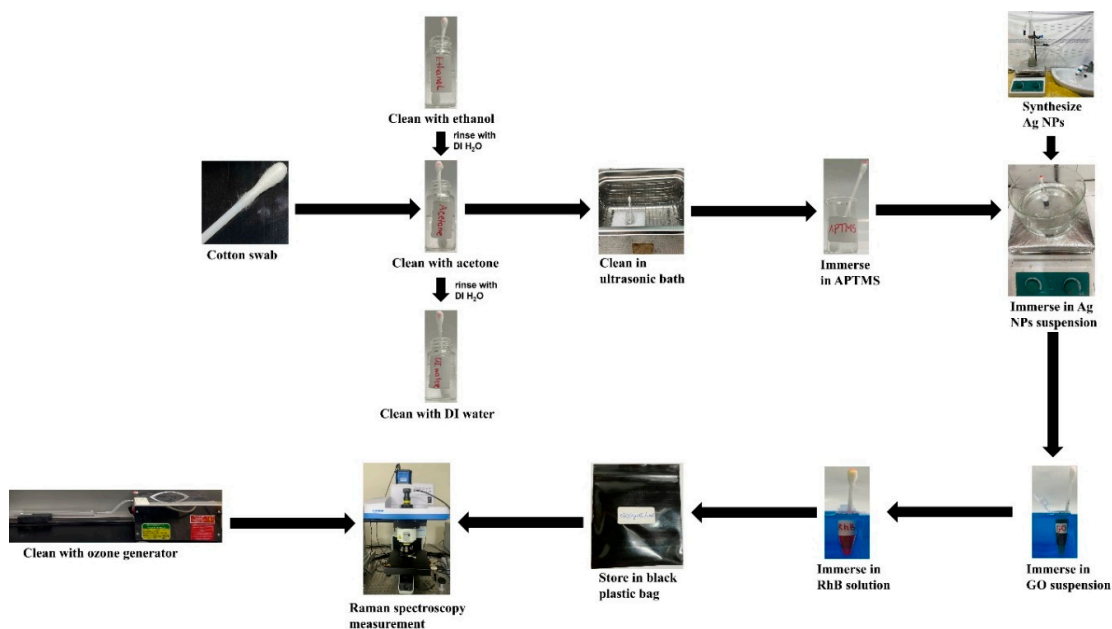


Figure 1. Illustration diagram showing key substrate fabrication and performance test steps.

For the synthesis of Ag NPs, we followed the reduction method described by Lee and Meisel [43], while GO nanosheets were synthesized according to the modified Hummers' method [44]. To fabricate SERS substrates, we followed the method recently reported by our group [29].

2.4. Performance Tests of SERS Substrates

For the sensitive detection of Rhodamine B (RhB) and thiophanate methyl (TM), we diluted RhB dye and high-purity thiophanate methyl ($C_{12}H_{14}N_4O_4S_2$, 98%), purchased from Acros Organics (Waltham, MA, USA) and Merck (Darmstadt, Germany), respectively, to DI water until reaching the desired concentrations. The SERS substrates were then dipped into RhB and TM solutions and subjected to laser irradiation of wavelength of 638 nm. SERS spectra were obtained from an XploRA Plus Raman Spectrometer (Horiba, UK), using 10x objective lens for three accumulations of 35s each. Signals from several random locations on each substrate were recorded to confirm homogeneity.

To assess the stability of Ag NPs/cotton swab and GO/Ag NPs/cotton swab, we placed each substrate in an uncovered container to expose each substrate to the ambient environment for periods of 6, 10, 11, and 12 months. At each specified time interval, the substrates were retrieved, rinsed with DI water, and dried at 120°C for 30 minutes, then immersed in RhB at 10^{-5} M and dried at room temperature for 15 min. This process was repeated four times before the samples were stored in black plastic food bags and subjected to Raman spectroscopy measurements.

To assess the recyclability of the substrate, GO/Ag NPs/cotton swab with 10^{-5} M RhB was placed inside a glass cylinder with one end sealed and the other end connected to an ozone generator nozzle (ZY-H135 GEN II, 3500 mg/h) operating at 230 V, 21 W power consumption and 50 Hz frequency. The ozone concentration in the glass cylinder was set at 25%. After one hour of exposure to the ozone environment, the GO/Ag NPs/cotton swab substrate was removed and analyzed using Raman spectrometer. Subsequently, the same GO/Ag NPs/cotton swab substrate was dipped again in 2ml of RhB at 10^{-5} M, then dried at room temperature for 15 min and subjected to Raman spectroscopy. This recyclability assessment process was repeated until no distinct peaks of RhB were observed.

3. Results and Discussion

3.1. Characterization of Cotton-Swab Based SERS Substrates

Figure 2 shows the cotton swab before and after the deposition of Ag NPs and GO nanosheets. Before the deposition, the surface of cotton swab was smooth (Figure 2(a)). After the deposition of Ag NPs (Figure 2(b)), the particles covered most of the surface area of cotton swab making it rougher. The Ag NPs were mostly quasi-spherical whose average size was estimated to be 65.76 ± 11.67 nm or 65.76 nm \pm 17.75%. The Ag NPs were well dispersed in DI water but upon deposition on cotton swab, they tended to agglomerate. The agglomeration assisted the formation of the deposition layer, made it thick and made it rough to generate more SERS hot spots. Clearly, the coverage was not dense, but Ag NPs were distributed throughout the entire surface of cotton swab. In Figure 2(c), we show a more magnified SEM image of the substrate after GO being added to better observe a thin layer of GO nanosheets covering most of the Ag NPs. Pt was deliberately included as a very thin coating layer to enhance the visibility of GO.

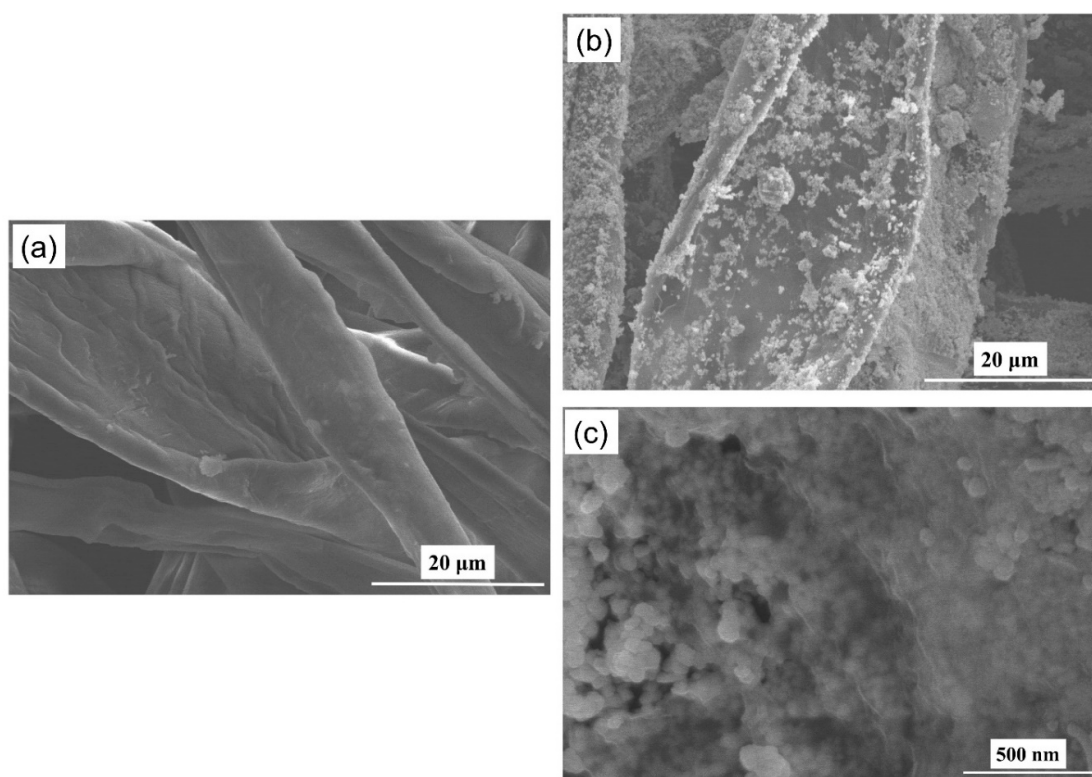


Figure 2. SEM images of (a) plain cotton swab, (b) Ag NPs/cotton swab, and (c) GO/Ag NPs/cotton swab.

The XRD pattern of Ag NPs was recorded directly on cotton swab by cutting a small portion of the sample and fixing it on the sample holder. As seen in Figure 3(a), the diffraction peaks at $2\theta \approx 38^\circ$, 44° , 65° , 78° and 82° were indexed as the constructive interferences of the reflected x-rays from the (111), (200), (220), (311) and (222) planes of the fcc crystalline Ag NPs. Furthermore, the two non-indexed peaks at $2\theta \approx 14^\circ$ and 23° were identified as those of the crystalline cellulose of the cotton strands [29]. No other peaks were observed indicating that the Ag NPs/cotton swab substrate was successfully fabricated without any interfering species or variants. We also utilized the available Raman spectrometer to provide further proof of the presence of GO on the surface as seen in Figure 3(b). In particular, two prominent Raman peaks of GO can be easily observed in the figure, one is at 1343 cm^{-1} assumed to be the D peak and one is at 1591 cm^{-1} assumed to be the G peak. Two small peaks at 471 cm^{-1} and 663 cm^{-1} could be assigned to the organic remnants on the surfaces of Ag NPs

after the synthesis. On the other hand, Raman spectrum of plain cotton swab, when compared with GO/Ag NPs/cotton swab, shows no noticeable peaks that could interfere with those of GO.

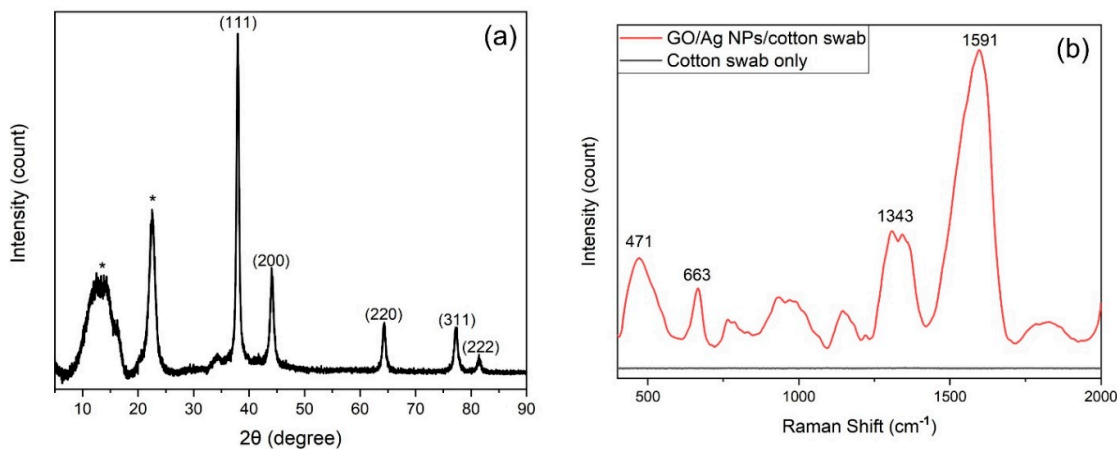


Figure 3. (a) XRD pattern of Ag NPs/cotton swab and (b) Raman spectra of GO/Ag NPs/cotton swab and plain cotton swab.

3.2. Performance of Cotton-Swab Based SERS Substrates in Detecting RhB and Thiophanate Methyl

We evaluated the performance of our cotton-swab based SERS substrates by using them to detect Rhodamine B (RhB) and thiophanate methyl (TM). RhB is an organic compound belonging to the xanthene group. While it is widely used as colorant in various industries including textile, paint, paper, glass, plastic and food, RhB when released to the environment is a dangerous contaminant due to its stability, developmental toxicity, mutagenicity and carcinogenic activities [45]. For SERS, RhB is a popular molecular probe due to its well-documented vibrational features. Multiple RhB concentrations ranging from 10^{-3} down to 10^{-12} M were prepared by diluting the stock solution multiple times until reaching the desired concentrations. Figure 4 presents our selected results showing an improved detection limit of 10^{-12} M RhB. Specifically, all eight prominent peaks of RhB at 620 cm^{-1} , 933 cm^{-1} , 1191 cm^{-1} , 1281 cm^{-1} , 1357 cm^{-1} , 1505 cm^{-1} , 1531 cm^{-1} and 1649 cm^{-1} were clearly observed for Raman spectra of higher RhB concentrations, from 10^{-3} M to 10^{-6} M (not shown). The list of major RhB peaks and their associated Raman mode assignments is shown in Table 1. At RhB concentrations of 10^{-8} M and below, some weaker peaks at 620 cm^{-1} , 1505 cm^{-1} and 1531 cm^{-1} started to die down with decreasing concentrations while other peaks remained visible even at 10^{-12} M. At these low concentrations, we also observed peak shifting toward either lower or higher wavenumbers as well as peak intensity fluctuation. We attributed these behaviours to the possible redistribution of charges and altered electronic molecular structure of RhB-Ag complex due to changing molecular interactions throughout such a wide range of RhB concentrations [46]. When comparing the performance of Ag NPs/cotton swab and GO/Ag NPs/cotton swab side by side, down to 10^{-8} M, we consistently observed higher peak intensities with the latter while other peak features remained unchanged. The addition of GO on top of Ag NPs clearly enhanced the sensitivity of the substrate due to its better adsorption of probe molecules, its supplementary chemical enhancement effect, and perhaps synergistic interactions with Ag NPs. From 10^{-10} M to 10^{-12} M, however, there was no noticeable difference in peak intensities with and without GO. At these ultra-low concentrations, the low populations of probe molecules made the contribution of GO surface to sensitivity insignificant. To the contrary, the Raman peaks obtained from Ag NPs/cotton swab substrates appeared sharper than those obtained from the substrates with GO. Likely, the diminishing SPR effect from Ag NPs when GO was laid in between Ag NPs and the probe molecules would dominate those advantages brought about by GO surface, reducing the overall sensitivity. When Raman spectrum of 10^{-3} M RhB was obtained from plain cotton swab without Ag NPs and GO, no obvious peak was detected

indicating that all the observable Raman peaks were enhanced exclusively by the presence of Ag NPs and GO nanosheets.

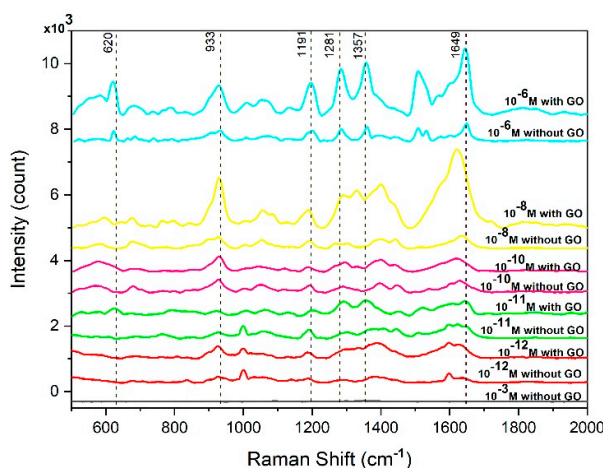


Figure 4. SERS sensitivity comparison between Ag NPs/cotton swab and GO/Ag NPs/cotton swab substrates at multiple RhB concentrations.

Table 1. Raman mode assignments for RhB.⁴⁷

Raman shift (cm ⁻¹)	Assignment
1644	Aromatic C-C stretch
1591	C-H stretch
1551	Aromatic C-C stretch
1528	C-H stretch
1508	Aromatic C-C stretch
1426	C-H stretch
1360	Aromatic C-C stretch
1284	Aromatic C-C stretch
1199	C-H in-plane bend
1130	C-H stretch
932	C-H stretch
773	C-H stretch
622	C-C-C stretch
355	
278	
240	Ag-N stretch
213	

Next, we applied the same detection method to thiophanate methyl (TM). It is a member of the benzimidazole group of fungicides, mainly used to control diseases caused by ascomycota fungal pathogen in vegetables. However, human exposure to TM would cause serious health effects such as skin disease, muscle twitching, and kidney or nervous system damaging. Therefore, TM is classified as a toxic agricultural chemical by the World Health Organization (WHO) and its maximum residue limit is set to the range of 0.05 – 5 mg/kg, depending on food category, by the Food and Agriculture Organization (FAO) [48]. It is, thus, important to be able to detect TM present in our agricultural products and ecological environment. A series of TM concentrations from 10⁻² M to 10⁻¹⁰ M in DI water was prepared as probe molecules. Cotton swab-based SERS substrates were dipped into each concentration and the corresponding Raman spectra were recorded and shown in Figure 5. Again, plain cotton swab substrate without any Ag NPs and GO showed virtually no peak even when 10⁻²

M TM was used, strongly confirming that cotton swab alone was a non-active SERS substrate. When Ag NPs, then GO was added to cotton swab, typical peaks of TM were easily spotted. Specifically, at the highest TM concentration, 10^{-2} M, nearly all of the reported Raman peaks showed up in our spectra with and without GO (Figure 5(a) & Table 2). Decreasing TM concentration reduced the number of TM peaks. In particular, from 10^{-4} to 10^{-6} M, the number of TM peaks was slightly reduced to those around 1600 cm^{-1} , 1480 cm^{-1} , $1200 - 1300\text{ cm}^{-1}$, 1000 cm^{-1} , $700 - 900\text{ cm}^{-1}$, and 650 cm^{-1} (Figure 5(a)). Then, from 10^{-8} M to 10^{-10} M, the number of TM peaks was reduced to only three peaks at 1589 cm^{-1} , $\sim 1180\text{ cm}^{-1}$ (double peaks), and 996 cm^{-1} (Figure 5(b)). Similar to RhB, we observed peak shifting, peak intensity fluctuation, and change of peak shape at high TM concentration range ($10^{-2}\text{ M} - 10^{-6}\text{ M}$) and we also attributed them to the concentration-dependent molecular interactions. By contrast, at the low concentration range ($10^{-8}\text{ M} - 10^{-10}\text{ M}$), the peaks appeared uniform with concentrations, perhaps due to sparse distribution of the TM molecules preventing them from mutual interactions. When comparing TM spectra from Ag NPs/cotton swab and GO/Ag NPs/cotton swab side by side, we observed no difference in peak intensities. It was not quite clear to us why GO didn't enhance TM peak intensity as it did with RhB. One possible explanation was the overwhelming electronic interactions between TM molecules that might dwarf the effect of charge transfer between GO and TM and depress peak intensity enhancement by chemical mechanism. One surprising result from our investigation was the unexpected increase in peak intensity when TM concentration decreased. According to Stair *et al* [49] and Muehlethaler *et al* [50], sample self-absorption occurred when the analytes absorbed both the incident radiation and the scattered radiation, resulting in attenuated Raman signal and peak intensity. If self-absorption indeed applied to our samples, it would explain the low peak intensities observed with high TM concentrations when TM molecules were in proximity to each other and could absorb light scattered from their neighbors. When TM concentration decreased, the effect of self-absorption would also decrease as more distant TM molecules would less likely absorb each other's signals. This inversely proportional relationship between peak intensity and concentration would be extremely helpful for applications in which trace amount of analytes needs to be detected.

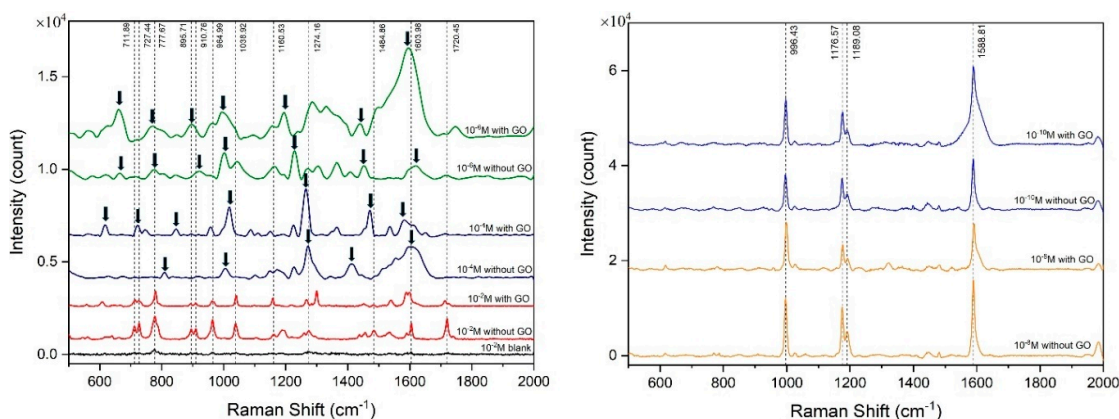


Figure 5. SERS performance comparison between Ag NPs/cotton swab and GO/Ag NPs/cotton swab substrates at TM concentrations of (a) $10^{-2}\text{ M} - 10^{-6}\text{ M}$ and (b) $10^{-8}\text{ M} - 10^{-10}\text{ M}$. The black arrows indicate TM peaks.

Table 2. Raman mode assignments for TM.^{51,52}

Raman shift (cm ⁻¹)	Assignment
325	C-C stretching
465	C-O-C deformation
613	-N-C=S deformation
717	C-H deformation, N-H bending

726	N-H wagging
779	C=S stretching, N-H deformation, C-H deformation
898	C-S stretching, C-H deformation
959	C=S stretching, C-H deformation
1039	C-H deformation, C-O stretching
1154	N-C-N asymmetric stretching, -CH ₃ deformation, C-C stretching
1267	C-O stretching, N-H deformation, C-H deformation
1298	C-O-C stretching, N-H deformation, C-H deformation
1538	C-N stretching, N-H deformation
1601	C=C stretching, N-H deformation, C-H deformation
1708	C=O stretching, N-H stretching, N-H deformation, -CH ₃ deformation

3.3. Investigation Based SERS Substrates

Among the plasmonic materials, Ag is dominantly the material of choice and has been used extensively in all kinds of morphologies and structures both commercially and in research. However, when Ag is exposed to air for sufficient time, it can be oxidized, turning metallic Ag⁰ into Ag⁺. The Ag₂O formed on the surface of Ag NPs would deactivate them as SERS substrates. Thus, while excellent sensitivity is the key characteristic that makes Ag so popular, the relatively quick degradation of this sensitivity over time in air, on the other hand, is an issue that makes Ag less attractive than Au, for example. In this work, we investigated the stability of Ag/cotton swab substrate in air, up to 12 months. Simultaneously, the stability of GO/Ag/cotton swab was also recorded for comparison. The results are shown in Figure 6. In addition, the average intensity ratios between peaks of Ag/cotton swab and GO/Ag/cotton swab are indicated in Figure 7 to give the readers an idea of how large the Raman signals obtained from one substrate were relative to those obtained from the other after each recorded month. Our first data set was obtained momentarily after the substrates were fabricated and, on average, the signal intensities from GO/Ag/cotton swab was ~1.5 times greater than those from Ag/cotton swab. Since many research groups chose a 6-month period or less to report their stability results, we decided to record our second data set after the same period to quickly reach the point that we expected significant degradation of Ag NPs. As seen in the figures, after 6 months, all the peaks obtained from Ag/cotton swab and GO/Ag/cotton swab had their intensities reduced. While this reduction made the spectrum harder to use to identify RhB by Ag/cotton swab, the reduction was much less severe for GO/Ag/cotton swab. In fact, after 6 months, the peak intensities obtained from the latter were, on average, still ~4.5 times greater than those obtained from the former. Ten months later, the RhB spectrum obtained from Ag/cotton swab was barely detectable and then no longer visible after 11 months and beyond. Likewise, although peak intensities did decrease in the RhB spectra of GO/Ag/cotton swab, even after 12 months, all eight prominent peaks of RhB were still somewhat detectable and consistently 3 times greater in intensities than those of Ag/cotton swab. Clearly, the results from this stability investigation encouraged the use of GO/Ag/cotton swab for longer shelf life of SERS substrate. We attributed this enhanced stability to the chemical enhancement mechanism described above, and to a much greater extent, to the protection of GO against Ag oxidation. If GO protection was not effective, RhB peak intensities would have decreased to the levels equivalent to those without GO after several months of air exposure because the Ag₂O formed would have deactivated the surfaces of Ag NPs, suppressing any synergistic GO-Ag NPs interactions and making the greater analyte adsorption of GO much less useful. Furthermore, if GO protection was not effective and Ag NPs were deactivated, the chemical enhancement mechanism alone would have not been able to maintain three times greater peak intensities for a RhB concentration of 10⁻⁵ M for almost a year. GO protection would have been more effective if GO completely covered Ag NPs which was not our case as seen in Figures 4(a),(b). More work on the relationship between the extent of GO coverage and the quality of its protection of Ag NPs from degradation by the ambient environment and the sampling environment will be conducted in the future.

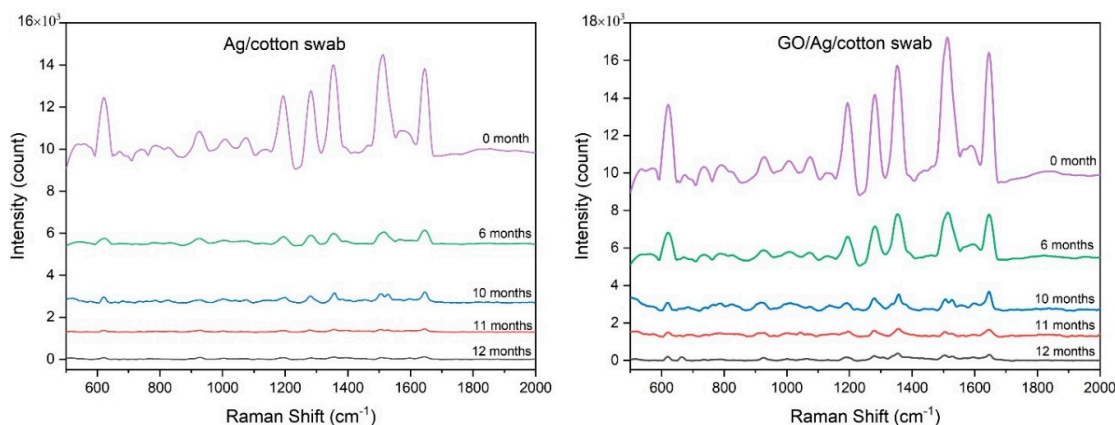


Figure 6. Degradation of RhB signals recorded after Ag/cotton swab and GO/Ag/cotton swab substrates were stored in air for up to 12 months. A RhB concentration of 10^{-5} M was used.

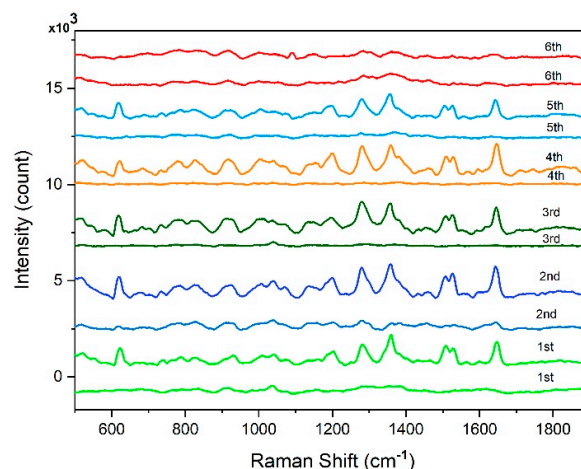


Figure 7. Average intensity ratios between peaks of GO/Ag/cotton swab and Ag/cotton swab over time from figure 6. The average intensity ratio at each recorded month was determined by dividing the intensity of each of the 6 prominent peaks of GO/Ag/cotton swab by the intensity of the corresponding peaks of Ag/cotton swab, then averaging them.

Regarding the recyclability of our SERS substrates, we decided to carry out our experiments with GO/Ag/cotton swab. We expected that the GO overlay would act as a shield to prevent Ag NPs from full attack of ozone, thus, keeping the surfaces of Ag NPs active longer for more detection cycles. Ozone has been used for more than a century as a disinfectant for drinking water and more recently has been used to treat inorganic and organic pollutants in wastewater. In the aquatic environment, gaseous ozone either forms hydroxyl radicals or directly reacts with microorganisms and pollutants to transform them into other unharmed species.⁵³ In this work, ozone reacted with RhB in vacuum and the results of multiple recycling rounds are shown in Figure 8. After the first round of RhB detection, the substrate was cleaned with ozone, and upon the treatment, Raman spectrum of the substrate surface was recorded for any trace of RhB left. As seen in Figure 8, no sign of RhB peak could be located. Then the same substrate was dipped again into 10^{-5} M RhB solution and we observed RhB peaks again this time without any noticeable reduction in intensity or the number of peaks or altering of peak shapes. Similar outcomes were also observed even after repeating this “on/off” cycles four more times for a total of five cycles. When we reached the 6th cycle, the substrate was still cleaned successfully without any trace of RhB, but this time no sign of RhB peaks was observed either after dipping the substrate in 10^{-5} M RhB. Thus, our results indicated that ozonation was a suitable method

to clean SERS substrates after RhB detection. The recyclability stopped at the 6th round could be due to two reasons. First, Ag NPs and GO could be deactivated completely at this stage. The abrupt decrease to zero signal at the 6th round instead of a gradual decrease in peak intensities indicated that there was a “surviving threshold” upon which Raman scattering enhancement collapsed and the substrate was deactivated. One possible scenario was that, after constantly exposing GO/Ag/cotton swab to ozone, the GO was eventually penetrated by ozone at the 6th round, leaving the entire surfaces of Ag NPs exposed to direct ozone oxidation and deactivated shortly after that. Second, rinsing the substrate after ozone cleaning didn't completely wash away the new transformed RhB products and they accumulated after each cycle. This accumulation of by-products would reduce the available substrate surfaces for RhB adsorption and weaken the Raman signals. The abrupt decrease to zero signal at the 6th recyclability round should be the result of those two degradation mechanisms combined. This ozonation method is expected to be applicable for cleaning other organic compounds as well and should be further explored.

Figure 8. Recyclability performance of GO/Ag NPs/cotton swab substrate showing five successful recycling rounds. A concentration of 10^{-5} M RhB was used.

4. Conclusions

Cotton-swab based SERS substrates, namely Ag/cotton swab and GO/Ag/cotton swab, were successfully fabricated using a facile solution-based method. We showed, in this work, that the cotton-swab based SERS substrates were ultra-sensitive by detecting RhB and thiophanate methyl at concentrations as low as 10^{-12} M and 10^{-10} M, respectively. We conducted further investigations on the stability and recyclability of these substrates and our results indicated that the GO/Ag/cotton swab substrate would still be able to detect RhB after 12 months exposed to the ambient environment and this GO/Ag/cotton swab substrate would be recycled up to five times by cleaning it with ozone. Regarding thiophanate methyl detection, we observed an increase in Raman peak intensities as the concentration of the analytes decreased, which proved to be very useful for detecting analytes of minute amount. In the near future, we expect to put our efforts toward exploring ways to improve the stability of the GO/Ag/cotton swab substrate and well as its recyclability. Different types of analytes to be detected will be also incorporated into our plan.

Author Contributions: Conceptualization, M.H.T.; methodology, M.H.T.; formal analysis, M.H.T., A.D.L, C.L.T.N. and M.D.H.; investigation, M.H.T., A.D.L, C.L.T.N., M.D.H. and K.V.T.; writing—original draft preparation, M.H.T; writing—review and editing, M.H.T; supervision, M.H.T. All authors have read and agreed to the published version of the manuscript.

Funding: This research is funded by Vietnam National University HoChiMinh City (VNU-HCM) under grant number C2022-20-23

Data Availability Statement: All data that support the findings of this study are included within the article

Conflicts of Interest: The authors declare no conflicts of interest.

References

1. Perez-Jimenez, A.I.; Lyn, D.; Lu, Z.; Liu, G.; Ren, B. *Chem Sci* **2020**, *11*(18), 4563-4577
2. Aragay, G.; Pino, F.; Merkoci, A. *Chem. Rev.* **2012**, *112*, 5317-5338
3. Xie, W.; Xu, A.; Yeung, E. *Anal. Chem.* **2009**, *81*, 1280-1284
4. Reisch, A.; Elpeleg, O.; Pon, L.; Schon, E. *Methods Cell Biol.* **2007**, *80*, 199-222
5. Patra, D.; Mishra, A. *Sens. Actuators B Chem.* **2001**, *80*, 278-282
6. Hill, H.; Simpson, G. *Field Anal. Chem. Technol.* **1997**, *1*, 119-134
7. Hoppmann, E.P.; Yu, W.W.; White, I.M. *Methods* **2013**, *63*, 219-224
8. Zhang, X.Y.; Young, M.A.; Lyandres, O.; van Duyne, R.P. *J. Am. Chem. Soc.* **2005**, *127*, 4484-4489
9. Nie, S.M.; Emory, S.R. *Science* **1997**, *275*, 1102-1106
10. Pieczonka, N.P.W.; Aroca, R.F. *Chem. Soc. Rev.* **2008**, *37*, 946-954

11. Sharma, B.; Frontiera, R.R.; Henry, A.I.; Ringe, E.; Van Duyne, R.P. *Mater. Today* **2012**, *15*(1-2), 16-25
12. Tran, M.; Roy, S.; Kmiec, S.; Whale, A.; Martin, S.; Sundararajan, S.; Padalkar, S. *Nanomaterials* **2020**, *10*(4), 644.
13. Dao, C.T.; Luong, N.T.Q.; Cao, A.T.; Kieu, M.N. *Comm. Phys.* **2019**, *29*(4), 521-526
14. Tran, M.; Whale, A.; Padalkar, S. *Sensors* **2018**, *18*(1), 147.
15. Liu, Z.; Yang, Z.; Cui, L.; Ren, B.; Tian, Z. *J. Phys. Chem. C* **2007**, *111*, 1770-1775.
16. Yu, X.; Cai, H.; Zhang, W.; Li, X.; Pan, N.; Luo, Y.; Wang, X.; Hou, J.G. *ACS Nano* **2011**, *5*(2), 952-958.
17. Ling, X.; Xie, L.; Fang, Y.; Xu, H.; Zhang, H.; Kong, J.; Dresselhaus, M.S.; Zhang, J.; Liu, Z. *Nano Lett.* **2010**, *10*, 553-561
18. Liu, Z.M.; Li, S.X.; Hu, C.F.; Zhang, W.; Zhong, H.Q.; Guo, Z.Y. *J. Raman Spectrosc.* **2013**, *44*, 75-80
19. He, R.; Lai, H.; Wang, S.; Chen, T.; Xie, F.; Chen, Q.; Liu, P.; Chen, J.; Xie, W. *Appl. Surf. Sci.* **2020**, *507*, 145116
20. Kim, J.; Jang, Y.; Kim, N.J.; Kim, H.; Yi, G.C.; Shin, Y.; Kim, M.H.; Yoon, S. *Front. Chem.* **2019**, *7*, 582
21. Sun, L.; Hu, H.; Zhan, D.; Yan, J.; Liu, L.; Teguh, J.S.; Yeow, E.K.L.; Lee, P.S.; Shen, Z. *Small* **2014**, *10*(6), 1090-1095
22. Mahmoud, A.Y.F.; Rusin, C.T.; McDermott, M.T. *Analyst* **2020**, *145*, 1396-1407
23. Im, H.; Bantz, K.; Lindquist, N.; Haynes, C.; Oh, S. *Nano Letters* **2010**, *10* (6), 2231-2236.
24. Wu, Y.; Hang, T.; Komadina, J.; Ling, H.; Li, M. *Nanoscale* **2014**, *6*, 9720-9726
25. Jiang, X.; Qin, X.; Yin, D.; Gong, M.; Yang, L.; Zhao, B.; Ruan, W. *Spectrochimica Acta Part a-Molecular and Biomolecular Spectroscopy* **2015**, *140*, 474-478.
26. Huang, L.; Zhou, Y.; Han, S.; Yan, Y.; Zhou, L.; Chen, W.; Zhou, P.; Chen, X.; Roy, V. *Small* **2014**, *10* (22), 4645-4650.
27. Tran, M.; Fallatah, A.; Whale, A.; Padalkar, S. *Sensors* **2018**, *18*(8), 2444
28. Gong, Z.; Du, H.; Cheng, F.; Wang, C.; Wang, C.; Fan, M. *Applied Materials & Interfaces* **2014**, *6*, 21931-21937
29. Hoang, M.D.; Nguyen, T.D.; Nguyen, C.T.L.; Luong, A.D.; Le, L.N.; Tran, K.V.; Huynh, K.C.; Nguyen, K.D.; Tran, M.H. *Mater. Res. Express* **2024**, *11*(2), 025002.
30. Kavitha, C.; Bramhaiah, K.; John, N.S.; Ramachandran, B.E. *Chem. Phys. Lett.* **2015**, *629*, 81-86.
31. Sun, S.; Wu, P. *Phys. Chem. Chem. Phys.* **2011**, *13*, 21116-21120
32. Ngo, D.X.; Tran, H.Q.; Le, V.V.; Le, T.T.; Le, T.A. *J. Sci.: Adv. Mater. Devices* **2016**, *1*, 84-89
33. Tran, H.T.; Nguyen, H.M.; Mai, H.H.; Pham, T.V.; Sai, D.C.; Nguyen, B.T.; Pham, H.N.; Nguyen, T.T.; Ho, H.K.; Nguyen, T.V. *VNU Journal of Science: Mathematics-Physics* **2020**, *36*(1), 1-6
34. Fang, H.; Zhang, C.X.; Liu, L.; Zhao, Y.M.; Xu, H.J. *Biosens. Bioelectron.* **2015**, *64*, 434-441
35. Kumar, S.; Lodhi, D.K.; Singh, J.P. *RSC Adv.* **2016**, *6*, 45120-45126
36. Xu, S.C.; Zhang, Y.X.; Luo, Y.Y.; Wang, S.; Ding, H.L.; Xu, J.M.; Li, G.H. *Analyst* **2013**, *138*, 4519-4525
37. Pham, T.N.; Le, H.X.; Dao, T.N.; Nguyen, L.T.; Binard, G.; de Marcillac, W.D.; Maitre, A.; Nguyen, L.Q.; Coolen, L.; Pham, N.T. *Appl. Phys. A* **2019**, *125*, 337
38. Gong, T.; Zhu, Y.; Zhang, J.; Ren, W.; Quan, J.; Wang, N. *Carbon* **2015**, *87*, 385-394
39. Xu, S.; Man, B.; Jiang, S.; Wang, J.; Wei, J.; Xu, S.; Liu, H.; Gao, S.; Liu, H.; Li, Z.; Li, H.; Qiu, H. *ACS Appl. Mater. Interfaces* **2015**, *7*(20), 10977-10987
40. Sun, L.; He, J.; An, S.; Zhang, J.; Ren, D. *J. Mol. Struct.* **2013**, *1046*, 74-81
41. He, X.; Wang, H.; Zhang, Q.; Li, Z.; Wang, X. *Eur. J. Inorg. Chem.* **2014**, *2014*(14), 2432-2439
42. Weng, X.; Feng, Z.; Guo, Y.; Feng, J.J.; Hudson, S.P.; Zheng, J.; Ruan, Y.; Laffir, F.; Pita, I. *New J. Chem.* **2016**, *40*, 5238-5244
43. Lee, P.C.; Meisel, D. *The Journal of Physical Chemistry* **1982**, *86* (17), 3391-3395.
44. Khai, T.V.; Long, L.N.; Khoi, N.H.T.; Thang, N.H. *Crystals* **2023**, *12*, 1825.
45. Priya, P.S.; Nandhini, P.P.; Vaishnavi, S.; Pavithra, V.; Almutairi, M.H.; Almutairi, B.O.; Arockiyaraj, S.; Pachaiappan, R.; Arockiaraj, J. *Comp. Biochem. Physiol. C Toxicol. Pharmacol.* **2024**, *280*, 109898.
46. Wang, Y.; Ji, W.; Sui, H.; Kitahama, Y.; Ruan, W.; Ozaki, Y.; Zhao, B. *J. Phys. Chem. C* **2014**, *118*, 10191-10197.
47. Zhixun, L.; Yan, F.; Jiannian, Y. *Trends in Applied Sciences Research* **2007**, *2*(4), 295-303
48. Food and Agriculture Organization of the United Nations. "Codex Pesticides Residues in Food Online Database." *Codex Alimentarius – International Food Standards*, <https://www.fao.org/fao-who-codexalimentarius/codex-texts/dbs/pestres/en/>. Accessed 12 December 2024
49. Wu, Z.; Zhang, C.; Stair, P.C. *Catal. Today* **2006**, *113*, 40-47.
50. Muehlethaler, C.; Lombardi, J.R.; Leona, M. *J. Raman Spectrosc.* **2017**, *48*(5), 647-652
51. Nguyen, H.T.N.; Le, T.N.T.; Nguyen, P.T.P.; Nguyen, H.D.; Nguyen, T.L.M. *Sensors* **2020**, *20*, 2229

52. Li, J.L.; Sun, D.W.; Pu, H. *Food Chem.* **2017**, *218*, 543-552.
53. Lim, S.; Shi, J.L.; von Gunten, U.; McCurry, D.L. *Water Res.* **2022**, *213*, 118053.

Disclaimer/Publisher's Note: The statements, opinions and data contained in all publications are solely those of the individual author(s) and contributor(s) and not of MDPI and/or the editor(s). MDPI and/or the editor(s) disclaim responsibility for any injury to people or property resulting from any ideas, methods, instructions or products referred to in the content.